

Research Article

IMM Filter Based Human Tracking Using a Distributed Wireless Sensor Network

Sen Zhang,¹ Wendong Xiao,¹ and Jun Gong²

¹ School of Automation and Electrical Engineering, University of Science and Technology Beijing, 30 Xueyuan Road, Haidian District, Beijing 100083, China

² School of Information and Science Engineering, Northeastern University, Shenyang 110031, China

Correspondence should be addressed to Wendong Xiao; wdxiao@ustb.edu.cn

Received 2 September 2013; Revised 21 November 2013; Accepted 1 December 2013; Published 8 January 2014

Academic Editor: Shuli Sun

Copyright © 2014 Sen Zhang et al. This is an open access article distributed under the Creative Commons Attribution License, which permits unrestricted use, distribution, and reproduction in any medium, provided the original work is properly cited.

This paper proposes a human tracking approach in a distributed wireless sensor network. Most of the efforts on human tracking focus on vision techniques. However, most vision-based approaches to moving object detection involve intensive real-time computations. In this paper, we present an algorithm for human tracking using low-cost range wireless sensor nodes which can contribute lower computational burden based on a distributed computing system, while the centralized computing system often makes some information from sensors delay. Because the human target often moves with high maneuvering, the proposed algorithm applies the interacting multiple model (IMM) filter techniques and a novel sensor node selection scheme developed considering both the tracking accuracy and the energy cost which is based on the tracking results of IMM filter at each time step. This paper also proposed a novel sensor management scheme which can manage the sensor node effectively during the sensor node selection and the tracking process. Simulations results show that the proposed approach can achieve superior tracking accuracy compared to the most recent human motion tracking scheme.

1. Introduction

In the daily life surveillance system, if the human actions can be tracked accurately, the results can help greatly and readily improve the ability of the identification of the whole system. Therefore, devices that can accurately track human motion in space are essential components of such a surveillance system. A complete model of human consists of both the movements and the shape of the body. Many of the available systems consider the two modeling processes as separate even if they are very close. In our study, the movement of the body is the target.

There have been some approaches to the human motion tracking. Most of the human motion tracking systems are based on vision sensors. The camera-based human tracking system is much more popular nowadays. Some of the proposed approaches present systems that are capable of segmenting, detecting, and tracking people using multiple synchronized surveillance cameras located far from each other. But they try to hand off image-based tracking from

camera to camera without recovering real-world coordinates [1–3]. Some other work has to deal with large video sequences involved when the image capture time interval is short [4, 5]. However, most vision-based approaches to moving human tracking are computationally intensive and costly expensive [6]. For example, they often involve intensive real-time computations such as image matching, background subtraction, and overlapping identification [6]. In fact, in many cases, due to the availability of prior knowledge on target motion kinematics, the intensive and expensive imaging detector array appears inefficient and unnecessary. For example, a video image consisting of 100×100 pixels with 8-bit gray level contains 80 kbits of data, while the position and velocity can be represented by only a few bits [7].

Recently wireless sensor network (WSN) technique has been developed quickly. A WSN consists of many low-cost spatially dispersed position sensor nodes. Each node can process information that it collected and received and exchange information with its neighboring nodes or the fusion center. Although there are many applications of WSNs on target

tracking [8–12], few papers can be found on human motion tracking in real-time systems [13, 14]. The recent proposed low-resolution camera-based WSNs for people tracking [15, 16] are still very computational and energy expensive. In this paper, we will develop an energy-efficient WSN technique for human motion tracking using low-cost ranging sensors.

Due to the limited resources of the sensor nodes for sensing, computation, and communication, the WSN will rely on collaborative information processing among sensor nodes to manage network resources and process the related information from different sensor nodes. Although various data fusion schemes and techniques have been proposed for combining measurements from many sensing nodes with limited accuracy and reliability, to achieve better accuracy and more robustness [14, 17, 18], the tracking accuracy is still limited due to the high maneuvering property of the human target. In this paper, an interacting multiple model (IMM) filter is employed to estimate the velocity and position of the human trajectory. IMM filter has the ability to switch between a high-process noise (or alternatively, higher order or turn) model in the presence of maneuvers and a low-process noise model in the absence of maneuvers. This gives the IMM filter its advantage over simpler estimators like the Kalman filter and extended Kalman filter (EKF). Based on the IMM filter, an adaptive sensor selection scheme is proposed in this paper for the tracking framework in order to save energy. Verified by simulations and a real testbed, the proposed algorithm can achieve more accurate estimation performance for human motion tracking compared to EKF [14].

The layout of the paper is arranged as follows. Section 2 presents the multiple models for human motion tracking. Section 3 presents the IMM estimator for our application. Section 4 proposes the sensor node selection method. Section 5 presents the simulation results and experimental results. Conclusions and future work are given in Section 6.

2. Problem Formulation

We consider the human moving in a 2D Cartesian coordinate system. The target state includes the human velocity, the human position in the coordinate, and the turn rate when the trajectory is along a curve. Assuming the human target has a nearly constant velocity and a nearly constant angular rate, we can build up the system models in this section.

2.1. Constant Velocity Model. Denote the human's position at time step k in the coordinate system as $(P_x(k), P_y(k))$, the velocity as $(V_x(k), V_y(k))$, and the sampling time interval as T . A constant velocity model that describes the human movement with a nearly constant velocity is

$$\mathbf{x}_1(k+1) = \mathbf{F}_1(\mathbf{x}_1(k)) + \mathbf{G}_1 \mathbf{v}_1(k), \quad (1)$$

where $\mathbf{x}_1(k) = [P_x(k) \ V_x(k) \ P_y(k) \ V_y(k)]^T$,

$$\mathbf{F}_1(\mathbf{x}(k)) = \begin{bmatrix} P_x(k) + T \cdot V_x(k) & V_x(k) & P_y(k) \\ +T \cdot V_y(k) & V_y(k) \end{bmatrix}, \quad (2)$$

and $\mathbf{v}_1(k)$ is the process noise which reflects possible imperfection of the assumption of the constant velocity. For convenience, we assume that \mathbf{v}_1 is a zero-mean Gaussian white noise with variance $\mathbf{Q}_1(k)$.

2.2. Coordinated Turn Model. In order to describe the human's more complex trajectory, such as turn left or turn right, here we adopt the coordinated turn model similar to [11]:

$$\mathbf{x}_2(k+1) = \mathbf{F}_2(\mathbf{x}_2(k)) + \mathbf{G}_2 \mathbf{v}_2(k), \quad (3)$$

where $\mathbf{x}_2(k) = [P_x(k) \ V_x(k) \ P_y(k) \ V_y(k) \ \omega(k)]^T$,

$$\mathbf{F}_2(\mathbf{x}_2(k)) = \begin{bmatrix} P_x(k) + \frac{\sin \omega(k) T}{\omega(k)} \cdot V_x(k) - \frac{1 - \cos \omega(k) T}{\omega(k)} \cdot V_y(k) \\ \cos \omega(k) T \cdot V_x(k) - \sin \omega(k) T \cdot V_y(k) \\ P_y(k) + \frac{1 - \cos \omega(k) T}{\omega(k)} \cdot V_x(k) + \frac{\sin \omega(k) T}{\omega(k)} \cdot V_y(k) \\ \sin \omega(k) T \cdot V_x(k) + \cos \omega(k) T \cdot V_y(k) \\ \omega(k) \end{bmatrix},$$

$$\mathbf{G}_2(K) = \begin{bmatrix} \frac{1}{2} T^2 & T & 0 & 0 & 0 \\ 0 & 0 & \frac{1}{2} T^2 & T & 0 \\ 0 & 0 & 0 & 0 & T \end{bmatrix}^T. \quad (4)$$

Here $\omega(k)$ is the unknown constant turn rate and $\mathbf{v}_2(k)$ is the process noise. Although the actual turn rate is not exactly a constant, we can assume that it is not changed in a very short time interval. For convenience, we assume that \mathbf{v}_2 is a zero-mean Gaussian white noise with variance $\mathbf{Q}_2(k)$.

Since the above model is nonlinear, the estimation of the state will be done via EKF when the IMM is applied during the subprediction for different models. This needs the linearization of the system model. Thus the Jacobian matrix $\text{Jaco}(k)$ of (3) is given by

$$\text{Jaco}(k) = \begin{bmatrix} 1 & \frac{\sin(\hat{\omega}(k) T)}{\hat{\omega}(k)} & 0 & -\frac{1 - \cos(\hat{\omega}(k) T)}{\hat{\omega}(k)} & f_{\omega_1}(k) \\ 0 & \cos(\hat{\omega}(k) T) & 0 & -\sin(\hat{\omega}(k) T) & f_{\omega_2}(k) \\ 0 & \frac{1 - \cos(\hat{\omega}(k) T)}{\hat{\omega}(k)} & 1 & \frac{\sin(\hat{\omega}(k) T)}{\hat{\omega}(k)} & f_{\omega_3}(k) \\ 0 & \sin(\hat{\omega}(k) T) & 0 & \cos(\hat{\omega}(k) T) & f_{\omega_4}(k) \\ 0 & 0 & 0 & 0 & 1 \end{bmatrix}, \quad (5)$$

where

$$\begin{aligned}
 f_{\omega 1}(k) &= \frac{\cos(\hat{\omega}(k)T)TV_x(k)}{\hat{\omega}(k)} + \frac{\sin(\hat{\omega}(k)T)V_x(k)}{\hat{\omega}(k)^2} \\
 &\quad - \frac{\sin(\hat{\omega}(k)T)TV_y(k)}{\hat{\omega}(k)} - \frac{-1 + \cos(\hat{\omega}(k)T)V_y(k)}{\hat{\omega}(k)^2}, \\
 f_{\omega 2}(k) &= -\sin(\hat{\omega}(k)T)TV_x(k) - \cos(\hat{\omega}(k)T)TV_y(k), \\
 f_{\omega 3}(k) &= \frac{\sin(\hat{\omega}(k)T)TV_x(k)}{\hat{\omega}(k)} + \frac{1 - \cos(\hat{\omega}(k)T)V_x(k)}{\hat{\omega}(k)^2} \\
 &\quad + \frac{\cos(\hat{\omega}(k)T)TV_y(k)}{\hat{\omega}(k)} - \frac{\sin(\hat{\omega}(k)T)V_y(k)}{\hat{\omega}(k)^2}, \\
 f_{\omega 4}(k) &= \cos(\hat{\omega}(k)T)TV_x(k) - \sin(\hat{\omega}(k)T)TV_y(k), \\
 R_1 &= \hat{x}_2(k)^2 + \hat{x}_3(k)^2 - 2\hat{x}_2(k)\hat{x}_3(k)\cos\gamma, \\
 R_2 &= \hat{x}_3(k)\cos\gamma - \hat{x}_2(k)\cos(2\gamma), \\
 R_3 &= \hat{x}_2(k) - \hat{x}_3(k)\cos\gamma, \\
 R_4 &= -\hat{x}_2(k)\hat{x}_3(k)\cos(2\hat{x}_1(k))\cos^2\gamma + \hat{x}_2(k)\hat{x}_3(k)\cos(2\gamma) \\
 &\quad + \cos\gamma[-\hat{x}_3(k)^2 + (\hat{x}_2(k)^2 + \hat{x}_3(k)^2)\cos^2\hat{x}_1(k) \\
 &\quad - \hat{x}_2(k)^2\cos 2\gamma].
 \end{aligned} \tag{6}$$

2.3. System Observation Model. Let $Z_j(k)$ denote the k -th measurement of the target at time step t_k if sensor j is used. The measurement model is given by

$$Z_j(k) = h_j(x(k)) + v_j(k), \tag{7}$$

where h_j is a (generally nonlinear) measurement function depending on sensor j 's measurement characteristic and parameters (e.g., its location). $v_j(k)$ is the measurement noise of sensor j which is assumed independent and to be zero-mean Gaussian white noise with covariance $R_j(k)$.

Based on the above velocity constant model, the coordinated constant turn model, and the system observation model, the interacting multiple model filter is applied to estimate the system state variable which includes the human's position coordinate and velocity.

2.4. IMM Filter. The basic IMM algorithm (one cycle) is as follows.

Step 1. We calculate the mixing probabilities and interaction between different models:

$$\begin{aligned}
 \mu_{i'|j'}(k|k) &= \frac{1}{\bar{c}_{j'}} P_{i'j'} \mu_{i'}(k), \\
 \bar{c}_{j'} &= \sum_{i'} P_{i'j'} \mu_{i'}(k),
 \end{aligned}$$

$$\begin{aligned}
 \hat{x}_{0j'}(k|k) &= \sum_{i'} \hat{x}_{i'}(k|k) \mu_{i'|j'}(k|k), \\
 P_{0j'}(k|k) &= \sum_{i'} \left\{ P_{i'}(k|k) + [\hat{x}_{i'}(k|k) - \hat{x}_{0j'}(k|k)] \right. \\
 &\quad \times [\hat{x}_{i'}(k|k) - \hat{x}_{0j'}(k|k)]^T \left. \right\} \\
 &\quad \times \mu_{i'|j'}(k|k).
 \end{aligned} \tag{8}$$

In these equations, $\mu_{i'|j'}(k|k)$ is the mixing probability at time k (the weights with which the estimates from the previous cycle are given to each filter at the beginning of the current cycle); $\hat{x}_{0j'}(k|k)$ and $P_{0j'}(k|k)$ are the mixed initial condition for mode-matched filter j' at time k ; $P_{i'j'}$ is the transition probability between mode i' and mode j' . $\mu_{i'}$ is the mode i' probability at time k .

Step 2. Prediction and filtering are as follows:

$$\begin{aligned}
 \hat{x}_{j'}(k+1|k) &= F_{j'} \hat{x}_{0j'}(k|k) + \Gamma_{j'}(k) \bar{v}_{j'}(k), \\
 P_{j'}(k+1|k) &= F_{j'} P_{0j'}(k|k) F_{j'}^T + \Gamma_{j'}(k) \\
 &\quad \times Q_j(k) \Gamma_{j'}(k)^T, \\
 \hat{x}_{j'}(k+1|k+1) &= \hat{x}_{j'}(k+1|k) + W_{j'}(k) \\
 &\quad \times r_{j'}(k+1), \\
 P_{j'}(k+1|k+1) &= P_{j'}(k+1|k) F_{j'}^T - W_{j'}(k) \\
 &\quad \times S_{j'}(k) W_{j'}(k)^T,
 \end{aligned} \tag{9}$$

where $\hat{x}_{j'}(k+1|k)$ and $P_{j'}(k+1|k)$ are the state estimate and its covariance in model-matched filter j' at time step $k+1$. $F_{j'}(k+1)$ is the Jacobin matrix of the system model j' .

The observation residual is

$$r_{j'}(k+1|k+1) = z(k+1) - \hat{z}_{j'}(k+1|k). \tag{10}$$

The measurement prediction is

$$\hat{z}_{j'}(k+1|k) = H_{j'}(k+1) \hat{x}_{j'}(k+1|k), \tag{11}$$

where $H_{j'}(k+1) \hat{x}_{j'}(k+1|k)$ is Jacobin matrix of the system observation model of sensor j' .

The residential covariance is

$$\begin{aligned}
 S_{j'}(k+1|k) &= H_{j'}(k+1) P_{j'}(k+1|k) \\
 &\quad \times H_{j'}(k+1)^T + R_{j'}(k+1), \\
 W_{j'}(k+1) &= P_{j'}(k+1|k) H_{j'}(k+1)^T \\
 &\quad \times S_{j'}(k+1)^{-1}.
 \end{aligned} \tag{12}$$

The likelihood function for filter j' is

$$\Lambda_{j'}(k+1) = N(r_{j'}(k+1); 0, S_{j'}(k+1)). \quad (13)$$

The mode j' probability at time k is

$$\mu_{j'} = \frac{1}{c} \Lambda_{j'}(k+1) \sum_{i'} P_{i'j'} \mu_{i'}(k), \quad (14)$$

where c is a normalizing factor. $\hat{x}_{j'}(k+1|k+1)$ and $P_{j'}(k+1|k+1)$ are the state estimate and its covariance in mode-matched filter j' at time $k+1$.

Step 3. Combination of the different mode update results is

$$\begin{aligned} \hat{x}(k+1|k+1) &= \sum_{j'} \hat{x}_{j'}(k+1|k+1) \mu_{j'}(k+1), \\ P(k+1|k+1) &= \sum_{j'} \left\{ P_{j'}(k+1|k+1) \right. \\ &\quad \left. + [\hat{x}_{j'}(k+1|k+1) - \hat{x}(k+1|k+1)] \right. \\ &\quad \left. \times [\hat{x}_{j'}(k+1|k+1) - \hat{x}(k+1|k+1)]^T \right\} \\ &\quad \times \mu_{j'}(k+1). \end{aligned} \quad (15)$$

In this paper for human motion tracking, we adopt 2 models in IMM to estimate the system state variable including the target's position coordinate and velocity, that is, the constant velocity model and the coordinated constant turn model introduced in Section 2.

3. Adaptive Sensor Selection Scheme

The sensor node selection scheme based on the IMM filter for maneuvering target tracking framework will be proposed in this section. We assumed that each sensor node can detect the human target and determine the range of the sensor node, and the locations of all the sensor nodes are known. The popular approach only selects the sensor nodes which are closest to the predicted human location as estimated by the estimator such as EKF [14]. One of the shortcomings of this "closest" node approach is that it does not consider its contribution to the tracking accuracy and the energy consumption quantitatively and simultaneously but simply selects the sensor nodes. Therefore, we proposed an adaptive sensor selection scheme in this paper, which is similar to the work in [19]. In our proposed method, IMM filter will be applied instead of EKF in order to avoid the maneuvering property of the human target. The approach jointly selects the next tasking sensor node and automatically determines the sampling time interval simultaneously based on both of the prediction of the tracking accuracy and tracking energy cost.

Tracking accuracy can be measured by various criteria, such as the trace and the determinant of the covariance matrix and Fisher information defined on the Fisher information matrix. In our proposed approach, the tracking accuracy

is reflected by tracking error $\phi(k)$ at time step k which is defined as the trace of the covariance matrix $P(k|k)$; that is,

$$\phi(k) = \text{trace}(P(k|k)). \quad (16)$$

Given a predefined threshold $\phi_0(k)$, the tracking accuracy at time step k is considered to be satisfactory if

$$\phi(k) < \phi_0(k); \quad (17)$$

otherwise it is considered to be unsatisfactory.

Energy consumption is a main consideration in this paper. We utilize the following energy model. If current sensor i selects sensor j as the next tasking sensor, then the total energy consumed by sensor i in transmission is

$$E_t(i, j) = (e_t + e_d r_{ij}^\alpha) b_c, \quad (18)$$

where e_t and e_d are decided by the specifications of the transceivers used by the nodes, r_{ij} is the distance between sensor i and sensor j , b_c is the number of bits sent, and α depends on the channel characteristics and is assumed to be time invariant. Energy consumed in receiving is

$$E_r(j) = e_r b_c, \quad (19)$$

where e_r is decided by the specification of the receiver of sensor j . The energy spent in sensing/processing data of b_s bits by sensor j is

$$E_s(j) = e_s b_s. \quad (20)$$

Therefore the total energy consumption is

$$E(i, j) = E_t(i, j) + E_r(j) + E_s(j). \quad (21)$$

In this paper, we will ignore the energy consumption for idling state of the node.

Suppose the current time step is k and the current tasking sensor is the sensor i which receives state estimation $\hat{x}(k-1|k-1)$ and estimation covariance matrix $P(k-1|k-1)$ of the time step $k-1$ from its parent tasking sensor. It first updates the state estimation by incorporating its new measurement $Z_j(k)$ using IMM algorithm described in Section 2. Then it uses the sensor scheduling algorithm to select the next tasking sensor j and the next sampling interval Δt_k such that the sensor j can undertake the sensing task at the time $t_{k+1} = t_k + \Delta t_k$. We suppose Δt_k should be in the range $[T_{\min}, T_{\max}]$, where T_{\min} and T_{\max} are the minimal and maximal sampling intervals, respectively. If sensor j is selected with the sampling interval Δt_k , its associated predicted objective function is defined as

$$J(j, \Delta t_k) = w \Phi_j(k) + (1-w) \frac{E(i, j)}{\Delta t_k}, \quad (22)$$

where $\Phi_j(k)$ is the predicted tracking accuracy according to the IMM algorithm, $E(i, j)$ is the corresponding predicted cost given by (21), is the averaged energy consumption over the period. $w \in [0, 1]$ is the weighting parameter used to balance the tracking accuracy and the energy consumption.

The sensors are scheduled in the following two tracking methods.

(1) After prediction, none of the sensors can achieve the satisfactory tracking accuracy using any sampling interval in T_{\min} and T_{\max} . In this case, Δt_k is set to the minimal sampling interval T_{\min} and the sensor is selected by

$$j^* = \arg \min_{j \in A} \{J(j, T_{\min})\}, \quad (23)$$

where A is the candidate sensors that can be selected by sensor i . Generally in (23), $w \neq 0$. The purpose of this mode is to drive the tracking accuracy to be satisfactory as soon as possible with consideration of the energy consumption.

(2) After prediction, at least one sensor can achieve the satisfactory tracking accuracy. In this case, the optimal $(j^*, \Delta t_k^*)$ is selected by

$$(j^*, \Delta t_k^*) = \arg \min_{j \in A^*, \Phi(j, k) \leq \Phi_0} \left\{ \frac{E(i, j)}{\Delta t_k} \right\}, \quad (24)$$

where A^* is the set of sensors that can achieve the satisfactory tracking accuracy. Equation (24) utilizes the objective function (22) with $w = 0$. The basic idea of this mode is that when the predicted tracking accuracy is satisfactory, the sensors and the sampling interval are selected according to the energy efficiency.

It is easy to see that information-driven sensor querying (IDSQ) [18] corresponds to the special case of the above adaptive sensor selection approach where the fast tracking approach mode is used in each time step (by set $\Phi_0 = 0$).

For simplification, we suppose the sampling interval is selected from predefined N values $\{T_t\}_1^N$ where $T_1 = T_{\min}$, $T_N = T_{\max}$, and $T_{t_1} < T_{t_2}$ if $t_1 < t_2$. In addition the set $\{T_t\}_1^N$ is selected such that its values can evenly divide the interval $[T_{\min}, T_{\max}]$ into $N - 1$ subintervals.

4. Sensor Node Management Scheme

If the static sensor nodes' location estimation is to be built incrementally as information is gathered from sensors, there is typically a need for a sensor node localization management process in order to prevent the heavy computational burden when the system state matrix is augmented. This process has the function of managing the information present in the knowledge base and possibly aiding the sensing process. Given the fact that computational resources are limited, an information management technique that reduces the stored data without sacrificing much information is required. To improve the applicability of a spatial description to a larger variety of scenarios, it should present the ability to iteratively adapt its geometry to application-specific requirements. The sensor node management process can be divided into three aspects in dynamic environments as follows.

(1) Adding observed sensor nodes: when a sensor node observed in the current scan cannot be matched to the existing sensor node list, a new sensor node is initialized.

(2) Removing redundant sensor nodes: if all static sensor nodes are included for updating the state, the computational

requirement will be high. Thus, redundant sensor nodes that have not been observed for a long time interval should be removed.

(3) Removing unstable sensor nodes: sensor nodes become unstable or obsolete if they move or become permanently occluded. For example, sensor nodes might be stationary for a long period of time and can be considered suitable sensor nodes. But if they move, they are unstable sensor nodes and should be removed from the sensor management scheme. Another case is that structural changes may occur in the environment, such as some static sensor nodes removing. In other cases an object might be placed in front of a sensor node, occluding it from view. For whatever reason, some sensor nodes may cease to exist and no longer provide useful information. These unstable sensor nodes should be deleted from the sensor management scheme.

After data association, if a sensor node cannot be matched to any existing sensor node in the map, it is considered as a new sensor node. The sensor node initialization is activated. Otherwise, this observation is used for the system update.

After a specified time interval, we shall check if this sensor node is still matched by any new coming observations during this period. If it is matched by none of the observations sensed from external sensors within the specified interval, this sensor node should be removed from the sensor node listing. Otherwise, this sensor node will still be kept in our system variables.

Finally, the sensing process can be improved if sensors are told where to look at. This directed sensing technique will naturally have benefits, such as to speed up the estimation process or to extract information about the environment in a predefined way.

5. Experimental Results

The human target is assumed to move in the $X - Y$ plane of the Cartesian coordinate frame and the ground truth trajectory consists of the curves and lines. The monitored field is $100 \text{ m} \times 150 \text{ m}$ and covered by 25 randomly placed sensors. It is assumed that the sensors can only collect the range measurements from the target. The sensors are placed randomly in the field. We assume the noise covariance $\sigma_j = 0.001$ for any sensor j in the covariance matrix of the process noise. We will apply the adaptive sensor scheduling algorithm presented in Section 3 in tracking a human object. The measurement model for sensor j is assumed as follows:

$$Z_j(k) = \sqrt{(x(k) - x_j(k))^2 + (y(k) - y_j(k))^2} + v_j(k), \quad (25)$$

where $(x(k), y(k))$ is the location of the human object, $(x_j(k), y_j(k))$ is the known position of sensor j , and $v_j(k)$ is the zero-mean Gaussian measurement noise with variance σ_j . In this simulation, we use the constant velocity model and the constant angular rate (coordinated turn) model explained in Section 2 as the target motion model. IMM filter and sensor selection scheme is applied to predict the trajectory.

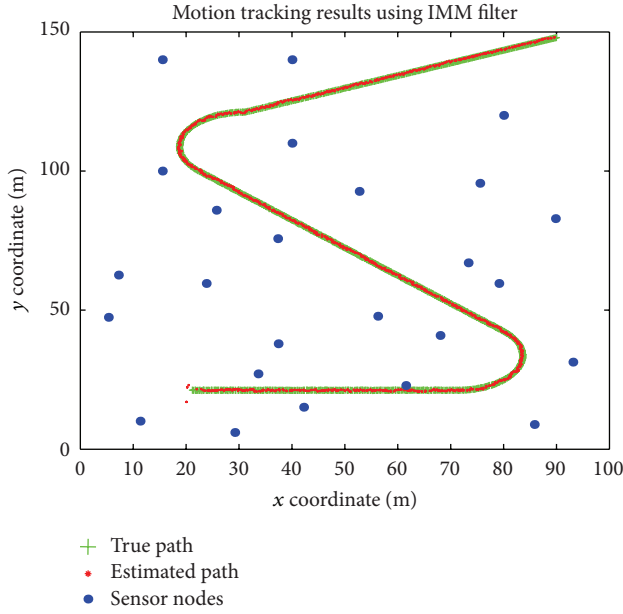


FIGURE 1: Human Motion Tracking Simulation Results Based on the Proposed Algorithm.

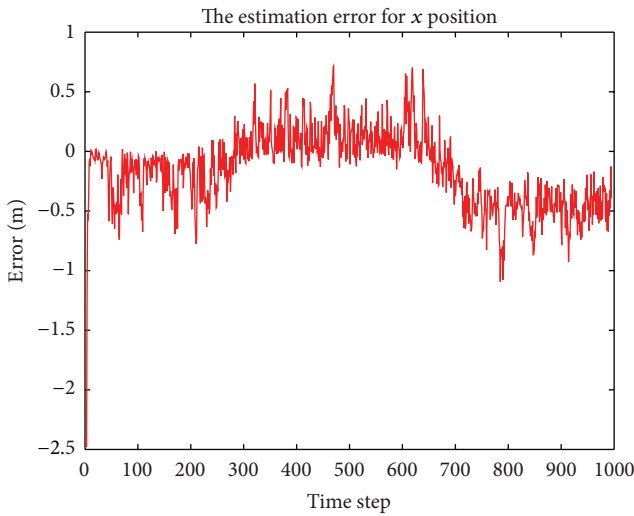


FIGURE 2: The estimation error between the ground truth of the trajectory and the predicted path.

The following parameter values taken from [20] are used in the energy model: $\alpha = 2$, $e_t = 45 \times 10^{-6}$, $e_r = 135 \times 10^{-6}$, $e_s = 50 \times 10^{-6}$, all in J/bit, and $e_d = 10 \times 10^{-9}$ in mJ/bit-m². In addition, b_c and b_s are assumed to be 1024. Thus in (21), $e_0 = 0.23552$ mJ and $e_1 = 1.024 \times 10^{-4}$ mJ/m².

For the sampling interval, we suppose $N = 5$, $T_{\min} = 0.1$, and $T_{\max} = 0.5$. We also assume $w = 0.16$ for the objective function (22) and the threshold of the tracking accuracy is set as $\Phi_0 = 2$.

Figure 1 shows the human tracking simulation results by the proposed IMM algorithm and range sensor nodes in the WSN. The green path means the ground truth we assumed

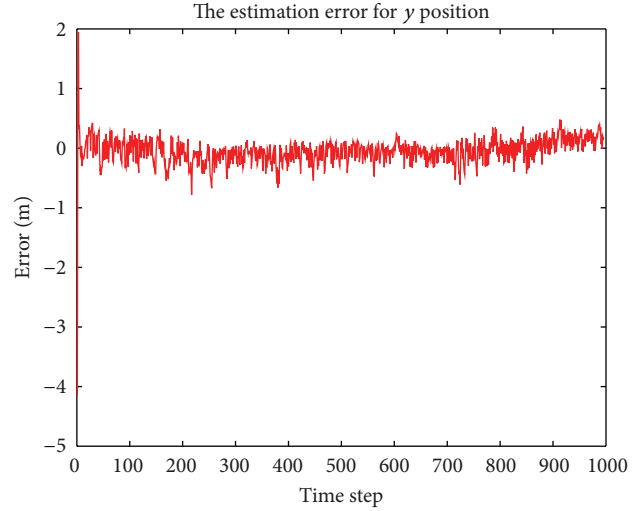


FIGURE 3: The estimation error between the ground truth of the trajectory and the predicted path.

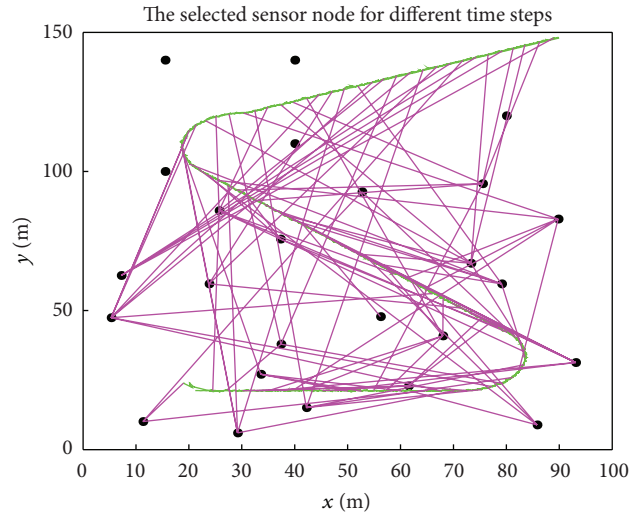


FIGURE 4: The selected sensor node for different time steps using the proposed sensor selection method.

and the red path is the estimation of the human trajectory. The blue points are the sensor nodes we randomly placed. Figures 2 and 3 give the estimation errors for Figure 1.

Figure 4 showed the sensor selected every ten steps during the target moving. The pink color line indicated the association of the selected sensor and the human position at that time step. We can see that a sensor can be chosen for several different steps.

We compare the performance of the proposed IMM based adaptive sensor scheduling scheme with the EKF based adaptive sensor scheduling scheme. Figures 5 and 6 showed the tracking accuracy comparison of the x coordinates and y coordinates when we use IMM filter and EKF together with the sensor selection method proposed in this paper. Clearly we can see that more accurate tracking accuracy is obtained when the IMM filter is used.

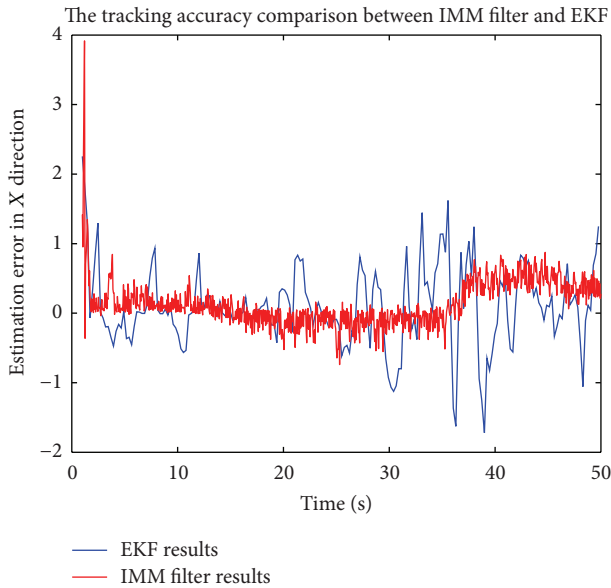


FIGURE 5: The x axis estimation error comparison of IMM filter and EKF.

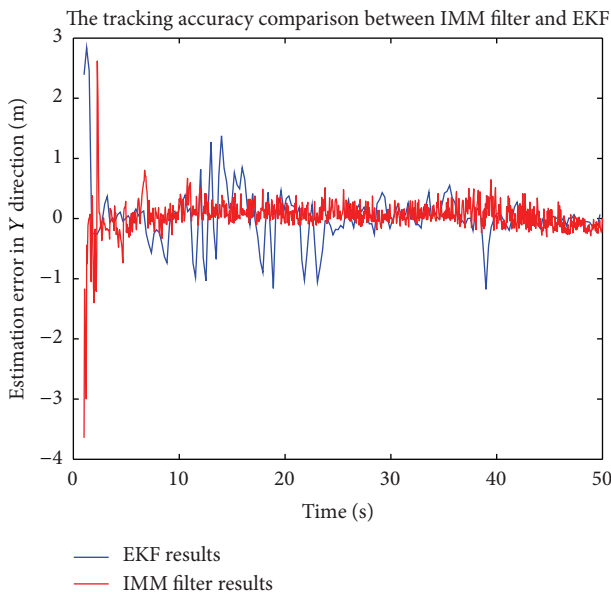


FIGURE 6: The y axis estimation error comparison of IMM filter and EKF.

6. Conclusions

This paper presented an IMM filter based human tracking approach and proposed an adaptive sensor scheduling scheme for the IMM filter based tracking framework in wireless sensor networks. The proposed method uses cheap range sensor nodes in wireless sensor networks by jointly selecting the next tasking sensor and determining the sampling interval based on predicted tracking accuracy and tracking cost under the IMM filter frame. Simulation results show that the new scheme can achieve significant

tracking accuracy considering the energy cost at each time step. Real testbed for human motion tracking is built up and the real time data implementation showed that the IMM filter based human motion tracking can give better results compared to the EKF based human motion tracking scheme. There are still many issues remaining for future study. Multistep, multisensor selection based adaptive sensor scheduling and sensor scheduling for multitarget tracking are both challenging problems for further investigations.

Conflict of Interests

The authors declare that there is no conflict of interests regarding the publication of this paper.

References

- [1] A. Mittal and L. S. Davis, "M2Tracker: a multi-view approach to segmenting and tracking people in a cluttered scene using region-based stereo," in *Proceedings of the European Conference on Computer Vision*, pp. 18–36, Copenhagen, Denmark, May 2002.
- [2] A. Mittal and L. S. Davis, "M2Tracker: a multi-view approach to segmenting and tracking people in a cluttered scene," *International Journal of Computer Vision*, vol. 51, no. 3, pp. 189–203, 2004.
- [3] M. Harville, "Stereo person tracking with adaptive plan-view statistical templates," in *Proceedings of European Conference on Computer Vision Workshop on Statistical Methods in Video Processing*, Copenhagen, Denmark, 2002.
- [4] Q. Cai and J. K. Aggarwal, "Tracking human motion in structured environments using a distributed-camera system," *IEEE Transactions on Pattern Analysis and Machine Intelligence*, vol. 21, no. 11, pp. 1241–1247, 1999.
- [5] T. Darrell, D. Demirdjian, N. Checka, and P. Felzenszwalb, "Plan-View trajectory estimation with dense stereo background models," in *Proceedings of the 8th IEEE International Conference on Computer Vision*, pp. 628–635, Vancouver, Canada, 2001.
- [6] W. Hu, T. Tan, L. Wang, and S. Maybank, "A survey on visual surveillance of object motion and behaviors," *IEEE Transactions on Systems, Man and Cybernetics C*, vol. 34, no. 3, pp. 334–352, 2004.
- [7] A. La Cour-Harbo, "Geometrical modeling of a two-dimensional sensor array for determining spatial position of a passive object," *IEEE Sensors Journal*, vol. 4, no. 5, pp. 627–642, 2004.
- [8] E. Mazor, A. Averbuch, Y. Bar-Shalom, and J. Dayan, "Interacting multiple model methods in target tracking: a survey," *IEEE Transactions on Aerospace and Electronic Systems*, vol. 34, no. 1, pp. 103–123, 1998.
- [9] D. Lu, Y. Yao, and F. He, "Sensor management based on cross-entropy in interacting multiple model kalman filter," in *Proceedings of the 2004 American Control Conference (AAC'04)*, pp. 5381–5386, Boston, Mass, USA, July 2004.
- [10] Q. Le, L. M. Kaplan, and J. H. McClellan, "Multiple-mode Kalman filtering with node selection using bearings-only measurements," in *Proceedings of the 36th IEEE Southeastern Symposium on System Theory (SSST'04)*, pp. 185–189, Atlanta, Ga, USA, 2004.
- [11] M. Mallick and B. F. La Scala, "IMM estimator for ground target tracking with variable measurement sampling intervals," in

- Proceedings of the 9th International Conference on Information Fusion (ICIF '06)*, pp. 1–8, Florence, Italy, July 2006.
- [12] P. S. Maybeck and B. D. Smith, “Multiple model tracker based on Gaussian mixture reduction for maneuvering targets in clutter,” in *Proceedings of the 8th International Conference on Information Fusion (ICIF '05)*, pp. 2043–2052, Florence, Italy, July 2005.
- [13] Q. Hao, D. J. Brady, B. D. Guenther, J. B. Burchett, M. Shankar, and S. Feller, “Human tracking with wireless distributed pyroelectric sensors,” *IEEE Sensors Journal*, vol. 6, no. 6, pp. 1683–1695, 2006.
- [14] Y. K. Toh, W. Xiao, and L. Xie, “A wireless sensor network target tracking system with distributed competition based sensor scheduling,” in *Proceedings of the 2007 International Conference on Intelligent Sensors, Sensor Networks and Information Processing (ISSNIP '07)*, pp. 257–262, Melbourne, Australia, December 2007.
- [15] A. Rahimi, B. Dunagan, and T. Darrell, “Tracking people with a sparse network of bearing sensors,” in *Proceedings of the 8th European Conference on Computer Vision*, pp. 507–518, Prague, Czech Republic, May 2004.
- [16] W. Zajdel, A. T. Cemgil, and B. J. A. Brose, “Dynamic Bayesian networks for visual surveillance with distributed cameras,” in *Proceedings of the 1st European Conference on Smart Sensing and Context*, pp. 240–243, Enschede, The Netherlands, 2006.
- [17] Y. Bar-Shalom, X. R. Li, and T. Kirubarajan, *Estimation with Applications to Tracking and Navigation*, John Wiley and Sons, 2001.
- [18] F. Zhao, J. Liu, L. Guibas, and J. Reich, “Collaborative signal and information processing: an information directed approach,” in *Proceedings of the IEEE Digital Object Identifier*, pp. 1199–1209, New York, NY, USA, 2003.
- [19] W. D. Xiao, J. K. Wu, L. H. Xie, and L. Dong, “Sensor scheduling for target tracking in networks of active sensors,” *Acta Automatica Sinica*, vol. 32, no. 6, pp. 922–928, 2006.
- [20] M. Bhardwaj and A. P. Chandrakasan, “Bounding the lifetime of sensor networks via optimal role assignments,” in *Proceedings of the 21st Annual Joint Conference of the IEEE Computer and Communications Societies (INFOCOM '02)*, pp. 1587–1596, New York, NY, USA, 2002.



Hindawi

Submit your manuscripts at
<http://www.hindawi.com>

